A R C H I W U M I N S T Y T U T U I N Ż Y N I E R I I L Ą D O W E J
Nr 12 ARCHIVES OF INSTITUTE OF CIVIL ENGINEERING 2012

STIFFNESS OF SHELLS WITH CONCRETE FILLED RIBS IN SOIL–STEEL BRIDGE STRUCTURES

Czesław MACHELSKI[*], Piotr TOMALA[**]
[*]) Ph.D., D.Sc, C.E. Wrocław University of Technology, Poland
[**]) M.Sc, C.E. ViaCon Polska sp. z o.o., Rydzyna, Poland

Abstract

Short and middle span soil-steel bridges are usually made of single corrugated overlapped plates. When the stiffness of a steel shell is not sufficient to carry the loads, additional plates (ribs) are used. They can be located either along the whole circumference or in some sectors only. Ribs are connected with the main shell by bolts. This connection is flexible even when the space between the shell and the ribs is filled with concrete, even if shear studs are used. In order to calculate internal forces in the elements of such a composite section, it is necessary to evaluate its stiffness. The value of connection stiffness may be assumed on the basis of results of load tests.

The paper presents analyses of efficiency of additional ribs filled with concrete (EC ribs). As a result of calculations values of deflection versus connection stiffness are given. The findings of these analyses may allow to estimate both the shell displacement during backfilling and values of internal forces under live loads. The paper proves that the connection stiffness depends on the load intensity also in the operational range.

Key words: soil-steel bridge, stiffness, layered shell, laboratory tests

1. INTRODUCTION

In 2005, in White Horse Creek, Alberta (Canada), on the area of a strip mine, the biggest soil-steel structure in the world with the span of L = 24 m [1] was built. The bridge was designed as a single radius structure made of SC 381×140×7.1 (length of corrugation × height of corrugation × plate thickness in [mm]) profiles. To obtain required stiffness during backfilling the structure was strengthened with concrete filled ribs (so called EC ribs) along the whole circumference [1]. Additionally the backfill material was reinforced with galvanized steel grids. These solutions allowed to reduce the shell uplift w, characterized [2] in the ratio w/L = 0.396 %. The soil-steel structure shown in Fig. 1 was

designed to carry an extremely heavy caterpillar of a total weight of 1144 tons [1]. It is a load which never occurs in typical road bridges.

Fig. 1. Soil-steel bridge in White Horse Creek [1]

At present the biggest soil-steel structure in Poland is the animal crossing built in 2007 over the electrified international railway line E20 (Berlin – Warsaw) in Gajec (Kunowice – Rzepin section). The structure was designed as a low arch with the span of L = 20 m, made of 381 × 140 × 7.1 profiles, strengthened by 381 × 140 × 5.5 plates, spaced every 1.524 m. This allowed to reduce the uplift ratio to w/L = 0.695 %.

To keep the designed geometry of the structure during backfilling, a suitable stiffness of the structure is needed. Small and middle span soil-steel arch structures are usually designed as shells without additional ribs. As the span length increses there is a need to add some extra cover plates to increase the stifness of the structure. In the case of largest spans the space between the main corrugated shell and corrugated cover plates is filled with concrete.

2. STIFFNESS OF A LAYERED SHELL

A parameter describing flexural stiffness EI_K of the main shell with a cover plate is the coefficient [3, 6]

$$\kappa = \frac{EI_K}{EI_b} \tag{1}$$

related to the main steel shell stiffness EI_b. In the case of a layered shell with no concrete filling it has two boundary values:

– maximal κ_{max} when connection presented in Fig. 2 is full

$$I_x = I_b + I_n + A_b \cdot a_b^2 + A_n \cdot a_n^2 , \tag{2}$$

– minimal κ_{min} when there is no composite action

$$I_x = I_b + I_n . \tag{3}$$

In the case of full cover plate made of the same steel profiles as the main shell ($I_b = I_n$, $A_b = A_n$) we receive a result from (2)

$$I_x = 2I_b + \frac{1}{2} A_b \cdot a^2 . \tag{4}$$

In the case of segmental cover plate made of the same profiles, when $I_b = 2I_n$ and $A_b = 2A_n$ we receive a result from (2)

$$I_x = \frac{3}{2} I_b + \frac{1}{3} A_b \cdot a^2 . \tag{5}$$

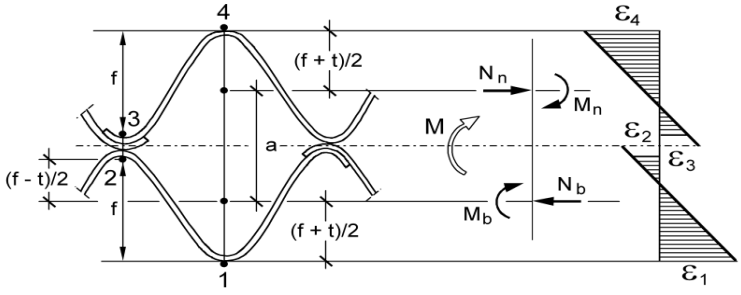

Fig. 2. Geometry, internal forces and strains in connected elements

On the basis of analyses given in [3] we obtain maximal span lengths L of the shells made of single corrugated plates SC ($\kappa = 1$). To obtain larger spans it is necessary to use additional cover plate of the same profile or with smaller plate thickness t ($4.5 > \kappa > 1$). Increment of the stiffness in the range of $6.6 > \kappa > 4.5$ is possible when a full cover plate (SC + SC) is used. The value of $\kappa > 6.6$ is possible when EC ribs filled with concrete are used (SC + C + SC), as in the example given in Fig. 1. Given ranges of κ were calculated assuming full main plate – cover plate interaction [3, 6].

3. INTERNAL FORCES IN COMPOSITE ELEMENT UNDER BENDING

When calculating the internal forces in the main shell and in the cover plate it is necessary to assume the connection stiffness of both elements [7]. For this

purpose the connection is tested under bending of the shell. In the paper partial interaction analyses on the basis of results of layered SuperCor corrugated plates laboratory tests [5] are presented.

In static analyses of composite layered structures the internal forces are distributed to the elements of the section [3, 6]. In the presented case global bending moment M is divided into forces acting in the main corrugated shell and in the ribbed cover plate. They are referenced to the centers of gravity of both elements of the cross-section. Their distance

$$a = f + \frac{3t}{2}. \tag{6}$$

is constant, as in Fig. 2

Figure 2 shows vertical dimensions of the cross-section and internal forces related to both elements (with n index to the ribbed cover plate and with b index to the main shell). Diagram of unit strains shows a discontinuity, depending on the connection stiffness C_z.

$C_z(x)$ value is used in calculations of composite girders using equation [3, 7]

$$\frac{E}{C_z}\frac{I_b + I_n}{a}\left(\frac{d^2N_b}{dx^2} - \frac{1}{C_z}\frac{dN_b}{dx}\frac{dC_z}{dx}\right) - \frac{I_x(A_b + A_n)}{aA_bA_n}N_b + M = 0\ , \tag{7}$$

where, according to Figure 3:

M – bending moment in the analyzed cross-section,

A_b, A_n – areas of cross-section elements,

I_b, I_n – moments of inertia of cross-section elements,

E = 205000 kN/m^2 – steel modulus of elasticity.

Based on the static condition follows that the force in the connection [3, 6] depends on the axial force N_b

$$T(x) = \frac{dN_b}{dx}. \tag{8}$$

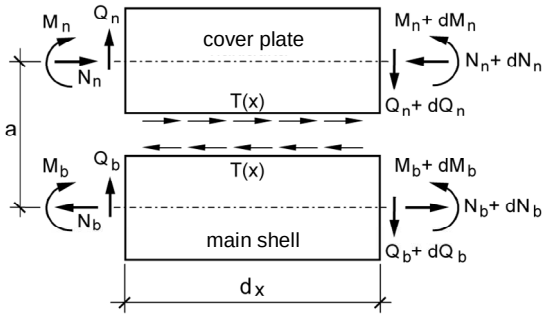

Fig. 3. Internal forces in a circumferential sector of a composite structure

Its value is very important in the design of a longitudinal connection between the main plate and the cover plate. If the space between these two plates is filled with concrete, the model of the layered structure (shown in Fig. 3) becomes more complex.

Shear studs used in EC ribs demand the introduction of two extra values of connection stiffness C_z as in (7). Despite the use of the same shear studs, connection stiffness will be different in concrete under compression and tension (compare Fig. 2). Physical properties of concrete may also be different in tension and compression zone. In order to estimate the influence of concrete filling on the stiffness of the shell, the comparison analysis based on the test results [5] is presented below.

4. TESTS OF LAYERED CORRUGATED PLATES

The circumferential connection between the main shell and the cover plate is assured by bolted joints. The aim of the presented study was to estimate effects of connection flexibility under loads occuring during construction and operation of a soil-steel structure.

Bending effects are analyzed using models of layered plates made of SC 381 × 140 × 7.1 profiles (Fig. 4). Static scheme of tested specimens is presented in Fig. 5. Configuration of plates in tested specimens P1 to P8 is described in [3, 5]. Main plate consisted of four profiles seamed longitudinally. Layout of cover plates was variable. All specimens were made of steel except for P4, made of aluminium. In elements P3 and P8 space between the main plates and ribs was filled with concrete. In elements P2, P3, P4 and P7 ribs were fully seamed (9 bolts per rib). Element P6 was typically connected (3 bolts per seam). During the testing (Fig. 4) the cover plate was placed under the main plate, inversely as in real shell structures.

Fig. 4. View of the tested plate P3 (EC ribs) [5]

Strains were measured in sections between applied forces and rows of bolts connecting the ribs. This section was marked as point 14 in Fig. 5. Deflections were measured in the middle of the span of tested specimens in three points along their width to check the priciples of bending of the plate to a cylindrical surface. The tests were carried out under load increments $2P$ = 25 kN.

5. PARAMETRICAL ANALYSIS

Figure 5 shows the static scheme of tested elements. It was assumed that the plates are under bending to a cylindrical surface, allowing to analyze a separated beam element. Beam deflection w_i in the middle point 15 (see Fig. 5) depends on the force value P and stiffness EI_K

$$w_i = \frac{Pc}{EI_K}\frac{3L^2 - 4c^2}{24} \tag{9}$$

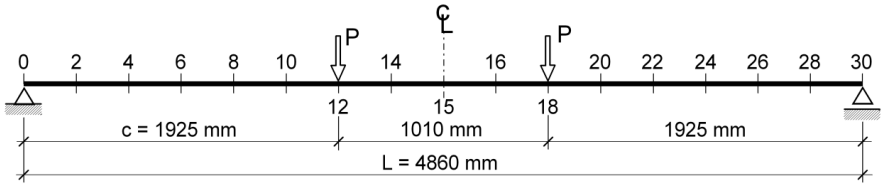

Fig. 5. Load scheme and section denotations in the element subjected to bending

If a constant stiffness EI_K along the beam length is assumed, formula (9) can be rewritten into

$$w_i = \frac{Pc}{24EI_b}\frac{3L^2 - 4c^2}{\kappa}\ , \tag{10}$$

when the coefficient (1) is taken into account. Using formula (10) the coefficient characterizing stiffness of a layered structure can be calculated on the basis of measured deflection w_i, related to the load value P and the main plate stiffness EI_b

$$\kappa = \frac{c\left(3L^2 - 4c^2\right)}{24EI_b}\frac{P}{w_i}\ . \tag{11}$$

The tested specimens of layered plates [5] were made of corrugated steel profiles SuperCor 381 × 140 × 7.1 (A_b = 9.81 mm^2/mm, I_b = 24164.6 mm^4/mm). The distance between the centres of gravity was a = 140 + 1.5 × 7.1

= 150.65 mm, according to (6). For the data mentioned above the moments of inertia were calculated to which the test results were related:

– from the formula (4)

$$I_x = I_b(2 + \frac{A_b \cdot a^2}{2 \cdot I_b}) = I_b(2 + \frac{9.81 \cdot 150.65^2}{2 \cdot 24164.6}) = 6.607\ \ I_b, \tag{12}$$

– from the formula (5)

$$I_x = I_b(1.5 + \frac{A_b \cdot a^2}{3 \cdot I_b}) = I_b(1.5 + \frac{9.81 \cdot 150.65^2}{3 \cdot 24164.6}) = 4.571\ \ I_b. \tag{13}$$

Figures 6 and 7 show diagrams of κ index versus load value 2*P*, calculated according to (11) for specimens with full cover plate (element P1) and filled with concrete (element P3). The range of κ index was limited to loads giving $w/L < 0.5$ % ratio. C_i is the number of a load cycle. Based on the diagram presented in Fig. 6 follows:

– in the first load cycle κ value rapidly decreases with load increment;
– κ value reached in the final stage of a load cycle increases in the subsequent load cycle.

The boundary value calculated according to (3) and (12), when there is no slip along the seam, is $\kappa_{max} = 6.607$ and when there is no connection $\kappa_{min} = 2.0$. Based on the diagram of κ coefficient given in Fig. 7 follows:

– κ value decreases along with load increment;
– κ value reached in the final stage of a load cycle decreases in the subsequent load cycle;
– κ values are higher when the EC ribs are used.

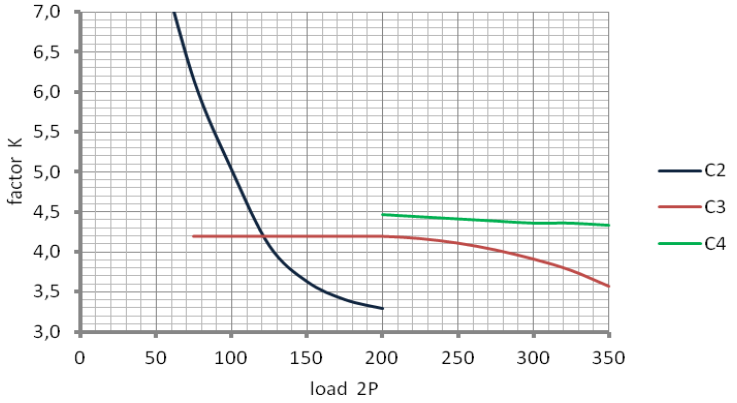

Fig. 6. Diagram of $\kappa(P)$ function, specimen P1 (full cover plate)

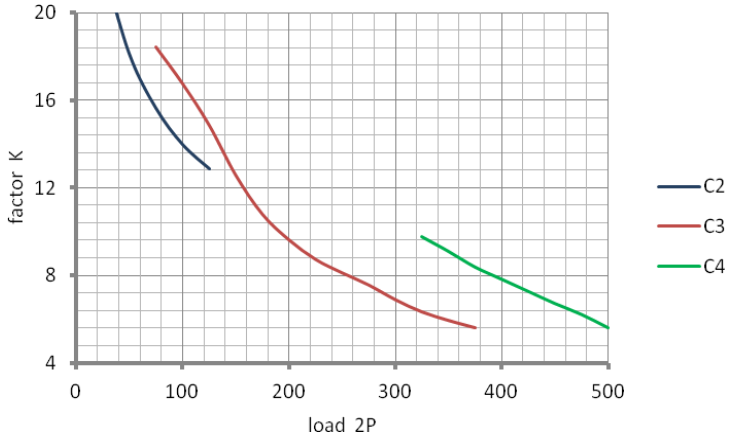

Fig. 7. Diagram of $\kappa(P)$ function, specimen P3 (full cover plate, EC ribs)

Figures 8 and 9 present diagrams of κ index, calculated on the basis of (11) for the load range giving w/L = 0.5 %. The analyzed cases were segmental cover plates as in element P5 and with EC ribs (specimen P8). The diagrams presented in Fig. 8 show similar relations as in the case of full cover, but when there is no seam slip we get κ_{max} = 4.57 as in (13) and when there is no connection from (3) we get κ = 1.5. Based on the results presented in Fig. 9 there follows a rather low efficiency of segmental cover, especially when the EC ribs filled with concrete are applied.

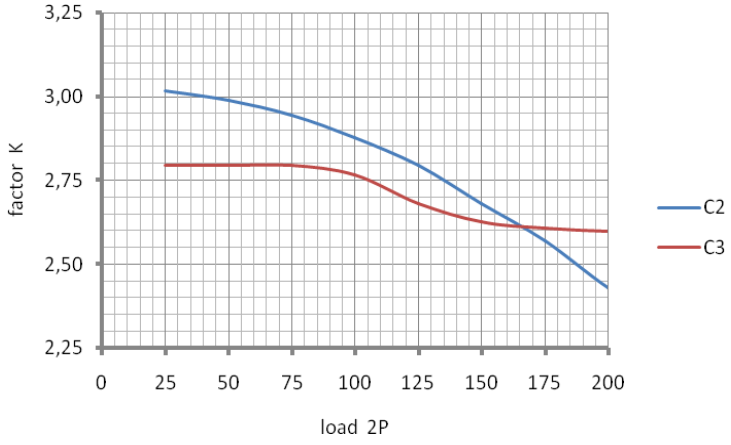

Fig. 8. Diagram of $\kappa(P)$ function, specimen P5 (segmental cover plate)

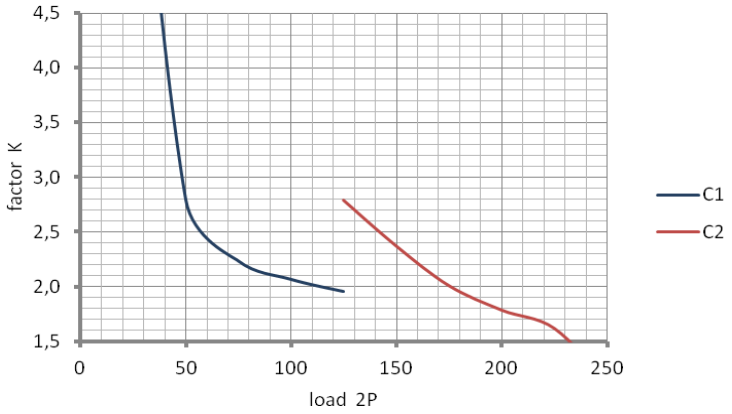

Fig. 9. Diagram of $\kappa(P)$ function, specimen P8 (segmental cover plate, EC ribs)

6. SUMMARY

To keep designed geometry of a soil-steel structure during construction a proper stiffness of a steel shell is required. Therefore in middle and large span structures it is necessary to use additional cover plates, connected with the main shell. In the case of largest spans the space between the main shell and cover ribbed plate is filled with concrete.

Connection of the main plate and ribs is flexible. Load tests of elements under bending prove that connection stiffness depends on the load intensity, also in the operational range. This paper describes method of estimating connection flexibility using κ coefficient. Presented results of analyses can be used to estimate the deflection of soil-steel shell structures during backfilling and to calculate internal forces distribution under live load.

REFERENCES

1. Bakht B.: *Evolution of the design methods for soil-metal structures in Canada*. Conference "Buried flexible steel structures". Archives of Institute of Civil Engineering, Poznań 1/2007, pp. 7-22.
2. Machelski C., Michalski J.B., Janusz L.: *Deformation Factors of Buried Corrugated Structures*. Journal of the Transportation Research Board, Solid Mechanic. Transportation Research Board of National Academies, Washington D.C. 8/2009, pp. 70-75.
3. Machelski C.: *Sztywność powłok warstwowych obiektów gruntowo-powłokowych* (*Stiffness of layered shells in soil steel bridge structures*). Drogi i Mosty, 4/2011.
4. Alexander A., Clifford L.: *Load test Report. Price Creek Culvert at Highway 11*. Bridge Office Engineering Standards Branch, April 2004.
5. Bakht B., Newhook J. P.: *Tests on SuperCor plates with different patterns of rib stiffening*. Final Report Atlantic Industries Limited, Canada November 2004.

6. Machelski C.: *Siły styczne w podatnym połączeniu elementów zginanych* (*Shear forces In flexible connection of bent elements*). Inżynieria i Budownictwo 12/2011, pp. 679-683.
7. Jeun S., Rhee J.: *An experimental verification of the improved bolting arrangement.* Conference "Buried flexible steel structures". Archives of Institute of Civil Engineering, Poznań 1/2007, pp. 109-119.
8. Machelski Cz.: *Deformacja stalowych powłok mostowych obiektów gruntowo-powłokowych podczas zasypki*. Geoinżynieria Drogi Tunele i Mosty, nr 06/2010.

SZTYWNOŚĆ POWŁOKI Z NAKŁADKĄ WYPEŁNIONĄ BETONEM W OBIEKCIE GRUNTOWO-POWŁOKOWYM

Streszczenie

Powłoki mostów gruntowo-powłokowych małych i średnich rozpiętości wykonuje się zwykle jako jednowarstwowe, z blach falistych łączonych na zakładkę. Gdy sztywność powłoki jest niewystarczająca, z uwagi na projektowany kształt powłoki lub jej rozpiętość, stosuje się nakładkę obwodową, w postaci pełnego płaszcza lub pasm odcinkowych. Połączenie nakładki odbywa się z użyciem śrub o rozstawie jak w powłoce podstawowej. Takie połączenie jest podatne również, gdy przestrzeń pomiędzy powłoką i nakładką wypełniona jest betonem, z użyciem dodatkowych łączników sworzniowych. Przy obliczaniu sił wewnętrznych w powłoce podstawowej i nakładce takiego układu warstwowego niezbędne jest założenie sztywności połączenia części składowych przekroju, tj. obydwu blach falistych i betonu. Wartość sztywności połączenia określa się na podstawie wyników badań.

W pracy przedstawiono analizę skuteczności połączenia obwodowego blach powłoki z nakładką, z zastosowaniem betonu wypełniającego, typu „EC ribs". Jako wyniki obliczeń podano ugięcia, w funkcji podatności połączenia. Wyniki tych analiz mogą służyć do szacowania przemieszczeń powłoki podczas zasypywania oraz obliczeń rozkładu sił wewnętrznych pod obciążeniami użytkowymi. Analizy podane w pracy wykazują, jak sztywność połączenia zależy od intensywności obciążenia, w zakresie obciążeń eksploatacyjnych.